HHS Public Access

Author manuscript

Magn Reson Med. Author manuscript; available in PMC 2018 October 01.

Published in final edited form as:

Magn Reson Med. 2017 October ; 78(4): 1452–1457. doi:10.1002/mrm.26509.

Repeatability of Magnetic Resonance Fingerprinting T1 and T2 Estimates Assessed Using the ISMRM/NIST MRI System Phantom

Yun Jiang[1], **Dan Ma**[2], **Kathryn E. Keenan**[3], **Karl F. Stupic**[3], **Vikas Gulani**[1,2], and **Mark A. Griswold**[1,2]

[1]Department of Biomedical Engineering, Case Western Reserve University, Cleveland, Ohio, United States

[2]Department of Radiology, Case Western Reserve University, Cleveland, Ohio, United States

[3]Physical Measurement Laboratory, National Institute of Standards and Technology, Boulder, Colorado, United States

Abstract

Purpose—The purpose of this study was to evaluate accuracy and repeatability of T_1 and T_2 estimates of a Magnetic Resonance Fingerprinting (MRF) method using the ISMRM/NIST MRI system phantom.

Methods—The ISMRM/NIST MRI system phantom contains multiple compartments with standardized T_1, T_2 and proton density values. Conventional inversion-recovery spin echo and spin echo methods were used to characterize the T_1 and T_2 values in the phantom. The phantom was scanned using the MRF-FISP method over 34 consecutive days. The mean T_1 and T_2 values were compared to the values from the spin echo methods. The repeatability was characterized as the coefficient of variation (CV) of the measurements over 34 days.

Results—T_1 and T_2 values from MRF-FISP over 34 days showed a strong linear correlation with the measurements from the spin echo methods ($R^2 = 0.999$ for T_1, $R^2 = 0.996$ for T_2). The MRF estimates over the wide ranges of T_1 and T_2 values have less than 5% variation, except for the shortest T_2 relaxation times where the method still maintains less than 8% variation.

Conclusion—MRF measurements of T_1 and T_2 are highly repeatable over time and across wide ranges of T_1 and T_2 values.

Keywords

MR Fingerprinting; quantitative imaging; relaxation time; repeatability; NIST system phantom

Correspondence: Mark Griswold, Ph.D., Case Western Reserve University, 11100 Euclid Ave - Bolwell B121, Cleveland, OH 44106, USA, mark.griswold@case.edu, Phone: +1-216-844-8085.

Introduction

Quantitative relaxometry shows promise for characterization and follow-up of disease in multiple clinical settings, such as neoplasm (1,2), multiple sclerosis (3,4), stroke (5), characterizing iron overload in liver (6), myocardial infarction (7), as well as monitoring treatment responses (8,9). However, the differences in T_1 and T_2 values between healthy and diseased tissues or between disease stages could be very small. To use quantitative relaxometry clinically, any variation in T_1 and T_2 measurement must be smaller than the differences between healthy and diseased tissues. Ideally the acquisition for measuring T_1 and T_2 values should be fast and accurate. It is also critical that measurements are highly repeatable, an important issue for tissue classification based on T_1 or T_2 values (10).

While many advances have been made to accelerate relaxometry (11–14), there are few studies (15,16) that assessed the repeatability of relaxometry methods. One reason is that these studies require phantoms with appropriate ranges of accurately known T_1 and T_2 values. These values should be stable over extended periods. An MRI system phantom was recently developed through the collaboration between the ISMRM Ad Hoc Committee on Standards for Quantitative Magnetic Resonance and the National Institute of Standards and Technology (NIST). The phantom has compartments containing solutions with a wide range of T_1 and T_2 values, and the solutions are well-characterized by NIST (17).

Magnetic Resonance Fingerprinting (MRF) is accurate and efficient in the simultaneous quantification of T_1 and T_2 by acquiring the transient-state signal with pseudo-random acquisition parameters (18–21). However, for these metrics to have clinical utility, the T_1 and T_2 values must be repeatable so that any observed difference in measured relaxivity between tissues or temporal change in measurement within a tissue can be assumed to be due to differences in physiology rather than scanner instability or methodological error. In this study, the repeatability of MRF derived T_1 and T_2 measurements in the ISMRM/NIST MRI system phatom is accessed over a period of 34 days.

Methods

ISMRM/NIST MRI System Phantom

The ISMRM/NIST MRI system phantom has multiple layers of sphere arrays that are designed to have a range of specific T_1, T_2 and proton density values. The spheres in the T_1 array are filled with $NiCl_2$ doped water, while the T_2 spheres are filled with $MnCl_2$ doped water. All solutions in the various compartments of the phantom are well-characterized by NIST and monitored by NIST for stability and accuracy (http://collaborate.nist.gov/mriphantoms/bin/view/MriPhantoms/MRISystemPhantom).

Gold Standard T_1 and T_2 Measurements by Spin Echo Methods

To characterize the T_1 and T_2 values in the system phantom, an inversion recovery spin echo (IR-SE) method and a multiple single-echo spin echo method were used on a Siemens 3T Skyra scanner (Siemens AG Healthcare, Erlangen, Germany).

T_1 measurements from the T_1 array were acquired by the IR-SE method with seven inversion times (TI) of 21 ms, 100 ms, 200 ms, 400 ms, 800 ms, 1600 ms and 3200 ms with a repetition time (TR) of 10000 ms, an echo time (TE) of 12 ms, a matrix size of 128 × 128, a field of view (FOV) of 17 cm, and a slice thickness of 5 mm. The scan time for each TI measurement was 21.3 minutes. The total scan time for the gold standard T_1 measurement was near 2.5 hours.

T_2 measurements from the T_2 array were obtained using a multiple single-echo spin echo method with seven TEs of 12 ms, 22 ms, 42 ms, 62 ms, 102 ms, 152 ms, and 202 ms, a TR of 10000 ms, a matrix size of 128 × 128, a FOV of 21 cm, and a slice thickness of 5 mm. The scan time of each TE measurement was 21.3 minutes. The total scan time the gold standard T_2 measurement was near 2.5 hours.

To calculate T_1 values, pixel-based nonlinear least-squares curve fitting was used to fit the magnitude of the IR-SE images to $S(TI) = a - be^{-TI/T_1}$. To calculate T_2 values, the magnitude values from the multiple single-echo spin echo images were fit to $S(TE) = ae^{-TE/T_2}$.

MR Fingerprinting Repeatability Measurements

The phantom was scanned on a Siemens Skyra 3T (Siemens AG Healthcare, Erlangen, Germany) with a 20-channel head-neck receiver array for 34 consecutive days to evaluate the repeatability of T_1 and T_2 estimates from the MRF method. For the daily measurement, the phantom was placed in the magnet for 30 minutes before the acquisition, to decrease the effects of motion on the measurements. The default global system adjustment was performed to adjust the B_0 shims and calibrate the RF power before MRF scans. No extra B_0 and B_1 mapping methods were performed in this study. A FISP-based MRF acquisition (19) was used to scan two slices, one through each of the T_1 and T_2 arrays, with an in-plane spatial resolution of 1.2 × 1.2 mm^2 and a slice thickness of 5 mm. Flip angles were varied between 5° – 75° and repetition times ranged from 12 to 15 ms (19). A total of 3000 frames were acquired for each slice, resulting in a scan time of 45 seconds per slice.

To compare the MRF method with the gold standard methods, the T_1 IR-SE method, the T_2 spin echo method, and MRF acquisitions through the T_1 and T_2 arrays were each repeated 5 times. The scan parameters were the same as described in the previous sections. The long acquisition time prohibited performing this measurement every day. The 5 repeated measurements were performed continuously, and the total acquisition time was about 25 hours.

MRF Reconstruction and Pattern Recognition

A dictionary containing a set of signal evolutions was generated by Bloch simulations. The dictionary resolution, denoted as min:step:max was [10:10:100, 120:20:1000, 1040:40:2000, 2050:100:3000] ms for T_1 and [2:2:10, 15:5:100, 110:10:300, 350:50:800] ms for T_2. The dictionary had a total of 4,141 entries that excluded unrealistic $T_2 > T_1$ combinations.

The undersampled spiral data were reconstructed using NUFFT (22) with a separately measured spiral trajectory (23,24). The coil sensitivity map was estimated using the Walsh

method (25) and derived from the average of the first 1000 coil-uncombined images. Pattern matching was performed by taking a complex dot product between the measured signal time course of each pixel and all entries of the dictionary. T_1 and T_2 values were derived from the entry that was maximally correlated against the acquired signal, and thus represented the closest dictionary entry to the acquired signal time course. NUFFT and pattern matching were implemented in the Siemens Image Calculation Environment (ICE, Siemens AG Healthcare, Erlangen, Germany). Twenty-five seconds were needed to reconstruct 3000 frames, estimate the coil sensitivity map, and combine the multiple coil images. The pattern matching process required 15 seconds using the current dictionary, for a 256 × 256 matrix acquisition.

Results

T_1 values estimated from IR-SE and T_2 values from the multiple single-echo spin echo technique are reported in Table 1. The mean and the standard deviation of each sphere were calculated from 50 pixels in a circular region-of-interest (ROI) that was manually drawn on the T_1 or T_2 map to exclude edge pixels.

Figure 1 shows T_1 (a) and T_2 (b) values of each sphere over 34 consecutive days of measurement. The T_1 and T_2 values were averaged over 70 pixels in a circular ROI drawn on T_1 and T_2 maps. Maps from MRF have higher spatial resolution compared to those from spin echo methods, allowing more pixels to be included in the ROI. The repeatability of T_1 (c) and T_2 (d) estimates from the MRF-FISP method is characterized as the coefficient of variation (CV), defined as the ratio of the standard deviation to the mean T_1 and T_2 values over 34 days. Over the wide ranges of T_1 and T_2 values, MRF estimates have less than 5 % variation, with the exception of T_2 relaxation times shorter than 13 ms, which shows a variation of 4.3–7.0 % (Figure 1c and 1d). The short T_2 relaxation times are on the order of the TR used for the MRF measurement.

Figure 2a shows the mean T_1 values obtained from MRF over 34 consecutive days plotted against those obtained from the gold standard IR-SE method. Figure 2b shows the mean T_2 values from MRF plotted against the values from the multiple single-echo spin echo method. The results show a strong linear correlation ($R^2 = 0.999$ for T_1, $R^2 = 0.996$ for T_2). The linear fits have slopes of 0.94 for T_1 values, 0.92 for T_2, and y-intercepts of -1.88 ms for T_1, and 7.28 ms for T_2.

Bland-Altman analysis was performed to assess the agreement between T_1 and T_2 values calculated from the MRF method and the values calculated from the spin echo methods. Figure 2c shows the Bland-Altman plot of T_1 values acquired with the IR-SE and the mean T_1 values obtained from MRF over 34 days. The mean bias for T_1 was 32.27 ms, and the 95% limits of agreement ranged from −46.13 ms to 110.68 ms. One data point with the longest T_1 value was outside of the limits of agreement. Figure 2d shows the Bland-Altman plot of T_2 values calculated from the multiple single-echo spin echo method and the mean T_2 values obtained from MRF over 34 days. The mean bias for T_2 was 3.66 ms, and the 95% limits of agreement ranged from −28.54 ms to 35.87 ms. Similarly, one data point with the longest T_2 value was outside of the limits of agreement.

The repeatabilities of the IR-SE method, spin echo method, and MRF method are shown in Figure 3. Over 5 repetitions, the IR-SE for T_1 estimation varied less than 0.2% for T_1 values larger than 30 ms and less than 1.3% for smaller T_1 values. The MRF results for T_1 estimation varied less than 1.3% for T_1 values larger than 40 ms and less than 2.3% for smaller T_1 values. For T_2 values larger than 20 ms, the variation of the spin echo method was less than 1.2 %, and the variation of MRF was less than 2.1%.

Discussion

MRF estimates of the wide range of T_1 and T_2 values in the ISMRM/NIST MRI system phantom varied less than 5% over 34 consecutive days . The mean T_1 and T_2 values over 34 days also showed strong linear correlation with the results from the gold standard T_1 and T_2 measurements. The longest relaxation times (both T_1 and T_2) were outside the Bland-Altman limits of agreement. This could be due to very long T_2 values in these spheres (> 500 ms) (17). Measurements of solutions with such long T_2 values are more susceptible to any system imperfections, such as inaccurate flip angles and the eddy current, etc.

While the gold standard spin echo methods showed better repeatability than the MRF method, the prohibitively long acquisition time of the spin echo method precludes its use in almost all clinical situations.

All methods showed greater variation in the shortest T_1 and T_2 values due to the choice of acquisition parameters in current experiment. The minimum TI in the IR-SE and the MRF method was 21 ms, which limited the ability to quantify T_1 values less than 21 ms accurately. The minimum TE used in the spin echo method was 12 ms, which limited the quantification of T_2 values that are on the order of the minimum TE. T_2 values on the order of the minimum TR used in the MRF method are the lower bound of accurate T_2 estimation.

The T_2 measurements had greater variation than the T_1 measurements, which could be a results of the B_1 variation from day to day. For the current study, the system default adjustment for the global B_0 and transmit radiofrequency power setting were used in the daily scan. No additional B_1 mapping was used to correct B_1 variation within the field-of-view. A previous MRF study (26) showed that B_1 variation affects the measured T_2 values more than T_1 values. Additional B_1 measurement and correction can improve the accuracy of the T_1 and T_2 estimates and should be included in cases where less than 5% variation is required. These variations could also be a result of small temperature fluctuations from day to day: the $MnCl_2$ solutions in the T_2 array are more sensitive to temperature changes than the $NiCl_2$ solutions in the T_1 array (27). A thorough study to examine the temperature dependence of the ISMRM/NIST MRI system phantom will be needed to address this issue.

The observed variations in T_1 and T_2 values could be affected by the dictionary resolution. In the current study, the shortest T_1 values, 21 ms and 32 ms, showed no variations. This was due to the T_1 value step size (10 ms) in the current dictionary. The dictionary resolution is a trade-off between the calculation time and the expected precision. A previous study (reported in the supplementary information of (18)) showed that the accuracy of the T_1 and T_2 estimates was not affected by the different dictionary resolutions, but the standard

deviations of the estimated T_1 and T_2 values were reduced when finer dictionary step sizes were used. This is a common result of almost any digital system in the presence of quantization noise; a higher precision in the quantization leads to higher precision in the final result. The repeatability observed in the current study could potentially be improved using a dictionary with a finer step size, though previous studies (18,20) have shown only minor improvements. In the current implementation of MRF, a straightforward template matching algorithm was utilized. This simple approach was used to rule out complications from the use of faster, but more complex algorithms. Higher repeatability could potentially be achieved without increasing the computation time by using a compressed dictionary (28,29) or other advanced processing algorithms.

Conclusion

Using the ISMRM/NIST MRI system phantom, MRF has high repeatability and accuracy over a period of 34 days across a wide range of T_1 and T_2 values.

Acknowledgments

Authors YJ, DM, VG and MAG acknowledge the NIH (1R01EB016728, 1R01EB017219, and 1R01DK098503) and Siemens Healthcare for grant support.

References

1. Just M, Thelen M. Tissue characterization with T1, T2, and proton density values: results in 160 patients with brain tumors. Radiology [Internet]. 1988; 169:779–85. DOI: 10.1148/radiology.169.3.3187000
2. Roebuck JR, Haker SJ, Mitsouras D, Rybicki FJ, Tempany CM, Mulkern RV. Carr-Purcell-Meiboom-Gill imaging of prostate cancer: quantitative T2 values for cancer discrimination. Magn Reson Imaging [Internet]. 2009; 27:497–502. DOI: 10.1016/j.mri.2008.08.001
3. Manfredonia F, Ciccarelli O, Khaleeli Z, Tozer DJ, Sastre-Garriga J, Miller DH, Thompson AJ. Normal-appearing brain t1 relaxation time predicts disability in early primary progressive multiple sclerosis. Arch Neurol [Internet]. 2007; 64:411–5. DOI: 10.1001/archneur.64.3.411
4. Papadopoulos K, Tozer DJ, Fisniku L, Altmann DR, Davies G, Rashid W, Thompson AJ, Miller DH, Chard DT. TI-relaxation time changes over five years in relapsing-remitting multiple sclerosis. Mult Scler [Internet]. 2010; 16:427–33. DOI: 10.1177/1352458509359924
5. Bernarding J, Braun J, Hohmann J, Mansmann U, Hoehn-Berlage M, Stapf C, Wolf KJ, Tolxdorff T. Histogram-based characterization of healthy and ischemic brain tissues using multiparametric MR imaging including apparent diffusion coefficient maps and relaxometry. Magn Reson Med [Internet]. 2000; 43:52–61.
6. St Pierre TG, Clark PR, Chua-anusorn W, Fleming AJ, Jeffrey GP, Olynyk JK, Pootrakul P, Robins E, Lindeman R. Noninvasive measurement and imaging of liver iron concentrations using proton magnetic resonance. Blood [Internet]. 2005; 105:855–61. DOI: 10.1182/blood-2004-01-0177
7. Ghugre NR, Ramanan V, Pop M, Yang Y, Barry J, Qiang B, Connelly KA, Dick AJ, Wright GA. Quantitative tracking of edema, hemorrhage, and microvascular obstruction in subacute myocardial infarction in a porcine model by MRI. Magn Reson Med [Internet]. 2011; 66:1129–41. DOI: 10.1002/mrm.22855
8. McSheehy PMJ, Weidensteiner C, Cannet C, Ferretti S, Laurent D, Ruetz S, Stumm M, Allegrini PR. Quantified tumor T1 is a generic early-response imaging biomarker for chemotherapy reflecting cell viability. Clin Cancer Res [Internet]. 2010; 16:212–25. DOI: 10.1158/1078-0432.CCR-09-0686
9. Weidensteiner C, Allegrini PR, Sticker-Jantscheff M, Romanet V, Ferretti S, McSheehy PMJ. Tumour T1 changes in vivo are highly predictive of response to chemotherapy and reflect the

number of viable tumour cells--a preclinical MR study in mice. BMC Cancer [Internet]. 2014; 14:88.doi: 10.1186/1471-2407-14-88

10. Moon JC, Messroghli DR, Kellman P, et al. Myocardial T1 mapping and extracellular volume quantification: a Society for Cardiovascular Magnetic Resonance (SCMR) and CMR Working Group of the European Society of Cardiology consensus statement. J Cardiovasc Magn Reson [Internet]. 2013; 15:92.doi: 10.1186/1532-429X-15-92
11. Schmitt P, Griswold MA, Jakob PM, Kotas M, Gulani V, Flentje M, Haase A. Inversion recovery TrueFISP: quantification of T(1), T(2), and spin density. Magn Reson Med [Internet]. 2004; 51:661–7. DOI: 10.1002/mrm.20058
12. Warntjes JBM, Dahlqvist O, Lundberg P. Novel method for rapid, simultaneous T1, T*2, and proton density quantification. Magn Reson Med [Internet]. 2007; 57:528–37. DOI: 10.1002/mrm.21165
13. Doneva M, Börnert P, Eggers H, Stehning C, Sénégas J, Mertins A. Compressed sensing reconstruction for magnetic resonance parameter mapping. Magn Reson Med [Internet]. 2010; 64:1114–20. DOI: 10.1002/mrm.22483
14. Ehses P, Seiberlich N, Ma D, Breuer FA, Jakob PM, Griswold MA, Gulani V. IR TrueFISP with a golden-ratio-based radial readout: fast quantification of T1, T2, and proton density. Magn Reson Med [Internet]. 2013; 69:71–81. DOI: 10.1002/mrm.24225
15. Siversson C, Tiderius C-J, Neuman P, Dahlberg L, Svensson J. Repeatability of T1-quantification in dGEMRIC for three different acquisition techniques: Two-dimensional inversion recovery, three-dimensional look locker, and three-dimensional variable flip angle. J Magn Reson Imaging [Internet]. 2010; 31:1203–1209. DOI: 10.1002/jmri.22159
16. Hannila I, Lammentausta E, Tervonen O, Nieminen MT. The repeatability of T2 relaxation time measurement of human knee articular cartilage. MAGMA [Internet]. 2015; 28:547–53. DOI: 10.1007/s10334-015-0494-3
17. Russek, SE., Boss, M., Jackson, EF., Jennings, DL., Evelhoch, JL., Gunter, JL., Sorensen, AG. Characterization of NIST/ISMRM MRI System Phantom. Proceeding 20th Annu. Meet. ISMRM; Melbourne, Victoria. Aust. 2012; p. 2456
18. Ma D, Gulani V, Seiberlich N, Liu K, Sunshine JL, Duerk JL, Griswold MA. Magnetic resonance fingerprinting. Nature [Internet]. 2013; 495:187–92. DOI: 10.1038/nature11971
19. Jiang Y, Ma D, Seiberlich N, Gulani V, Griswold MA. MR fingerprinting using fast imaging with steady state precession (FISP) with spiral readout. Magn Reson Med [Internet]. 2015; 74:1621–31. DOI: 10.1002/mrm.25559
20. Jiang Y, Ma D, Jerecic R, Duerk J, Seiberlich N, Gulani V, Griswold MA. MR fingerprinting using the quick echo splitting NMR imaging technique. Magn Reson Med [Internet]. 2016; doi: 10.1002/mrm.26173
21. Hamilton JI, Jiang Y, Chen Y, Ma D, Lo WC, Griswold M, Seiberlich N. MR fingerprinting for rapid quantification of myocardial T1, T2, and proton spin density. Magn Reson Med. 2016; doi: 10.1002/mrm.26216
22. Fessler JA, Sutton BP. Nonuniform fast fourier transforms using min-max interpolation. IEEE Trans Signal Process [Internet]. 2003; 51:560–574. DOI: 10.1109/TSP.2002.807005
23. Zhang Y, Hetherington HP, Stokely EM, Mason GF, Twieg DB. A novel k-space trajectory measurement technique. Magn Reson Med [Internet]. 1998; 39:999–1004. DOI: 10.1002/mrm.1910390618
24. Duyn JH, Yang Y, Frank JA, van der Veen JW. Simple correction method for k-space trajectory deviations in MRI. J Magn Reson [Internet]. 1998; 132:150–3. DOI: 10.1006/jmre.1998.1396
25. Walsh DO, Gmitro AF, Marcellin MW. Adaptive reconstruction of phased array MR imagery. Magn Reson Med [Internet]. 2000; 43:682–90.
26. Chen Y, Jiang Y, Pahwa S, Ma D, Lu L, Twieg MD, Wright KL, Seiberlich N, Griswold MA, Gulani V. MR Fingerprinting for Rapid Quantitative Abdominal Imaging. Radiology [Internet]. 2016; 279:278–286. DOI: 10.1148/radiol.2016152037
27. Keenan, K., Stupic, K., Boss, M., et al. Multi-Site, Multi-Vendor Comparison of T1 Measurement Using ISMRM/NIST System Phantom. Proceeding 24th Annu. Meet. ISMRM; Singapore. 2016. p. 3290

28. McGivney DF, Pierre E, Ma D, Jiang Y, Saybasili H, Gulani V, Griswold MA. SVD compression for magnetic resonance fingerprinting in the time domain. IEEE Trans Med Imaging [Internet]. 2014; 33:2311–22. DOI: 10.1109/TMI.2014.2337321

29. Cauley SF, Setsompop K, Ma D, Jiang Y, Ye H, Adalsteinsson E, Griswold MA, Wald LL. Fast group matching for MR fingerprinting reconstruction. Magn Reson Med [Internet]. 2015; 74:523–528. DOI: 10.1002/mrm.25439

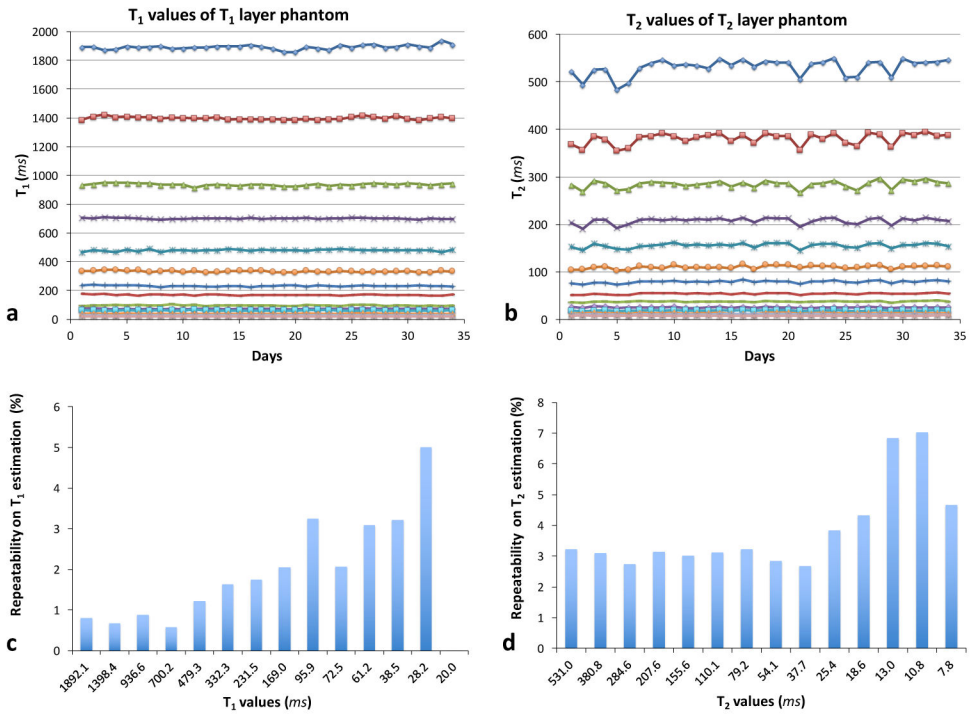

Figure 1.

T_1 (a) and T_2 (b) values of each sphere over 34 consecutive days. The repeatability of MRF-FISP T_1 (c) and T_2 (d) estimates is the standard deviation normalized by the mean T_1 and T_2 values of 34 days.

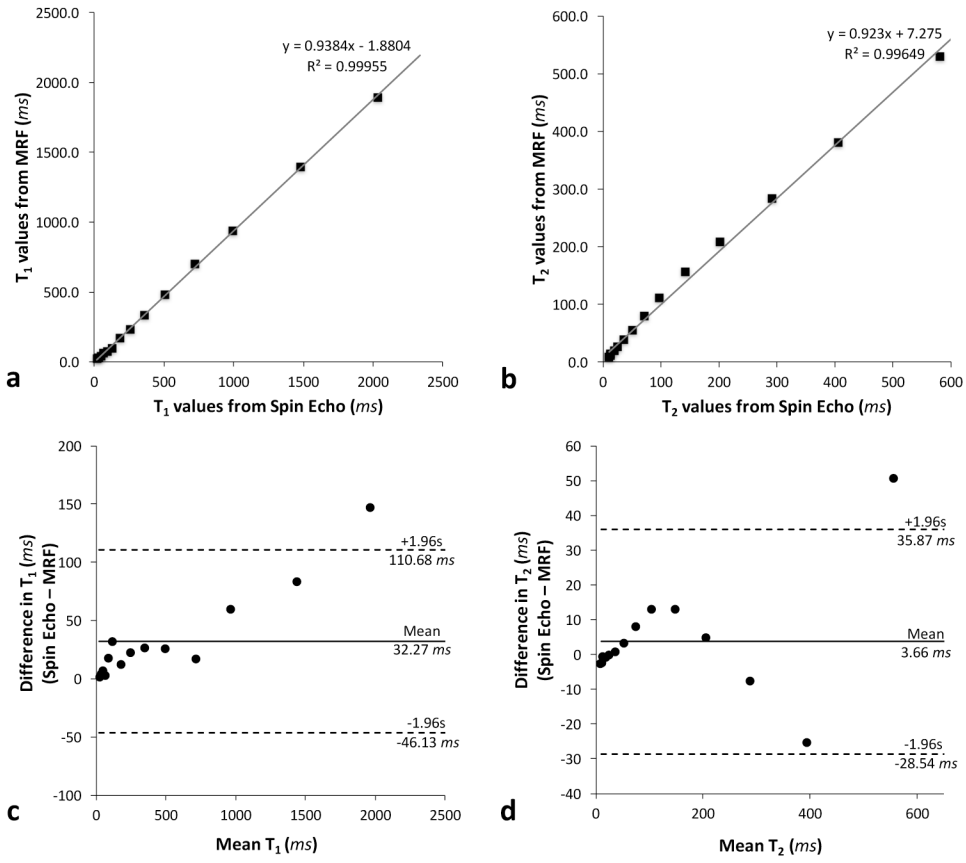

Figure 2.

Correlation plots (a–b) and Bland-Altman plots (c–d) comparing T_1 and T_2 values averaged over 34 consecutive days of MRF measurements to the T_1 and T_2 values obtained from the inversion recovery spin echo and spin echo methods, respectively.

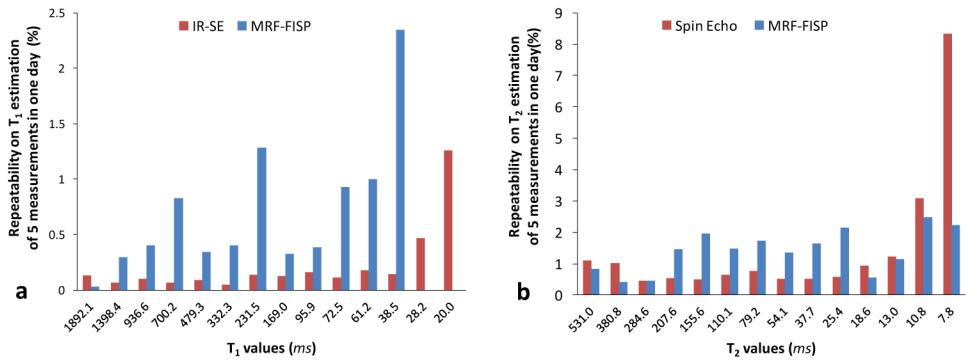

Figure 3.

The repeatability of T_1 (a) and T_2 (b) estimates from MRF-FISP method and the gold standard spin echo methods for each sphere (five repeated measurements).

Table 1

The mean and standard deviation (SD) of T_1 values estimated from inversion recovery spin echo measurements and T_2 values estimated from multiple single-echo spin echo measurements. The mean and standard deviation of each sphere were calculated from 50 pixels within a circular region-of-interest (ROI) that was manually drawn on the T_1 or T_2 map.

		1	**2**	**3**	**4**	**5**	**6**	**7**	**8**	**9**	**10**	**11**	**12**	**13**	**14**
T_1 (*ms*)	Mean	2038	1482	996	717	505	358	253	181	127	90	64	45	32	21
	SD	126	41	23	20	8	6	4	8	3	2	1	2	4	7
T_2 (*ms*)	Mean	581	406	292	203	143	97	71	51	37	26	20	14	13	11
	SD	22	15	16	10	9	3	7	5	5	3	5	2	10	6